

# Coincidence Factors for Domestic EV Charging from Driving and Plug-in Behavior

**Bollerslev, Jacob; Andersen, Peter Bach; Jensen, Tue Vissing; Marinelli, Mattia; Thingvad, Andreas; Calearo, Lisa; Weckesser, Tilman**

*Published in:*
IEEE Transactions on Transportation Electrification

*Link to article, DOI:*
10.1109/TTE.2021.3088275

*Publication date:*
2022

*Document Version*
Peer reviewed version

# Coincidence Factors for Domestic EV Charging from Driving and Plug-in Behavior

Jacob Bollerslev, *Student Member, IEEE*, Peter Bach Andersen, *Member, IEEE*, Tue Vissing Jensen, Mattia Marinelli, *Senior Member, IEEE*, Andreas Thingvad, *Student Member, IEEE*, Lisa Calearo, *Student Member, IEEE*, and Tilman Weckesser, *Senior Member, IEEE*

***Abstract*—This study models the coincidence factor (CF) of EV charging given driving and plug-in behaviors by combining data sources from travel surveys and recorded EV charging data. From these we generate travel and plug-in behaviors by using a Monte Carlo approach to derive coincidence factors. By varying EV battery size, rated charging power and plug-in behavior, their influence on the coincidence factor is examined. The key results show that the coincidence factor decreases to less than 25% when considering more than 50 EVs with a charging level of 11 kW, with the coincidence factor strongly depending on the number of EVs considered. By contrast, driving behavior and battery size have a minor influence on the coincidence factor. Further, when mixing the parameters, such as EV battery size and rated charging power, then especially the active power drawn by the feeder does not change linearly. Ultimately, the study aims to add to the state-of-the-art by solely and systematically focusing on the CF and its sensitivity to a number of key factors. For planning and design, distribution system operators may use this study as a part of their planning for integration of electric vehicles in the electrical grid.**

***Index Terms*—Electric Vehicles, Power system analysis, System analysis and design, Vehicle-Grid Integration, Coincidence factor, Charging simultaneity**

## NOMENCLATURE

*a) Abbreviations:*

**EV** Electric Vehicle
**SOC** State of charge (rel. to capacity)
**SSE** Sum of squared errors
**CF** Coincidence factor
**TU** The Danish National Travel Survey
**DSO** Distribution System Operator

*b) Sets:*

| | |
|---|---|
| $T$ | Time steps in simulation |
| $D$ | Days in simulation |
| $B_s$ | Set of batches for scenario $s$ |
| $R_b$ | Set of runs in batch $b$ |
| $V_r$ | Set of EVs in run $r$ |
| $J$ | Set of journeys in database |
| $S$ | Set of scenarios |

*c) Parameters:*

| | |
|---|---|
| $\eta$ | Performance ($\mathrm{km}$ driven per $\mathrm{kWh}$) |
| $l_j$ | Distance of journey $j$ in km |
| $\Delta SOC_j^{\text{used}}$ | Energy(SOC) usage during a journey |
| $e_s$ | Rated battery capacity for scenario |
| $r_s$ | Rated charging power for scenario |
| $SOC^{\text{low}}$ | State of charge at which an EV charges off-site during a journey |
| $E^{\text{offsite}}$ | Increase in state of charge per off-site charging event |
| $\hat{\gamma}_s, \hat{k}_s, \hat{c}_s$ | Fitted parameters for coincidence factor model for scenario $s$ |
| $M_b$ | Number of EVs in batch $b$ |

*d) Variables:*

| | |
|---|---|
| $SOC_{v,d}^{\text{arrival}}$ | SOC upon arrival at home for EV $v$ on day $d$ |
| $SOC_{v,d}^{\text{departure}}$ | SOC remaining upon departure from home for EV $v$ on day $d$ |
| $\Delta SOC_{v,d}^{\text{offsite}}$ | Total amount of energy recharged during the journey for EV $v$ on day $d$ |
| $\Delta t_{v,d}^{\text{charge}}$ | Charging time to fully recharge EV |
| $cf_b$ | Coincidence factor for batch $b$ |
| $P_r(t)$ | Power drawn from feeder in run $r$ at time $t$ |
| $\gamma, k, c$ | Coincidence factor model fit parameters |
| $\sigma$ | Standard deviation of max. CF |
| $\mu$ | Mean of max. CF |

*e) Functions:*

| | |
|---|---|
| $cf_b(M_b)$ | Model output coincidence factor from batch $b$ for $M_b$ EVs |
| $cf_s(M\|\gamma, k, c)$ | Fitted coincidence factors for number of EVs $M$ in scenario $s$ |
| $P_s^{\text{peak}}(M)$ | Peak active power draw for number of chargers $M$ in scenario $s$ |

## I. INTRODUCTION

With several countries seeking to phase out sale of non-electric vehicles over the coming years [1], energy needs for transportation will increasingly be covered by the electrical grid. Subsequently, the grid faces not only higher demand, but a demand that is concentrated depending on the charging locations available and the behavior of drivers. These factors could cause a rise in the coincidence factor of loads, requiring additional investments in grid infrastructure [2].

For system operators it is crucial to understand how the roll-out of electrified transportation will reflect in grid requirements over the coming decade. As a large part of the demand is expected to come from the residential sector

J. Bollerslev, P. B. Andersen, T. V. Jensen, M. Marinelli, A. Thingvad, and L. Calearo are with the Centre for Electric Power and Energy, Department of Electrical Engineering, Technical University of Denmark, Denmark.

T. Weckesser is with Danish Energy, Frederiksberg C, Denmark.

Corresponding author: Jacob Bollerslev, address (email: s163909@student.dtu.dk).

[3], which simultaneously requires the most costly grid reinforcement, characterizing the impact of electric vehicle (EV) adoption for residential load is especially pertinent.

To address this concern, a model of how residential EV coincidence factor (CF) depends on both driving behavior and the technical composition of charging infrastructure and EVs is needed. While many comprehensive studies have already been done on grid impacts of EV charging, [4–6], very few studies have an explicit and specific focus on the CF itself. As such, the CF's sensitivity to model inputs is typically underexplored, with models not capturing the full range of parameters impacting charging power requirements.

To fill this gap, we develop a model of EV charging which includes a wider range of factors than previously studied. The model uses driving patterns based on a database of user-reported travel behavior, plug-in behavior from real-world charging events, and a widened range of model parameters. We systematically consider the sensitivity of coincidence factors to EV parameters, and show how our method extends to combinations of these parameters. Further, we present methods for systematically deriving CFs from such models in a way that corrects for the inherent uncertainty of capturing population parameters.

The remainder of the paper is organized as follows. In Section II, we outline the findings of previous studies on EV user behavior and coincidence factors of EVs.Section III introduces our model for calculating the CF and describe the model parameters and inputs, while section IV describes considerations made for the implementation of the model. Based on the results presented in section V, we provide recommendations in section VI for policy and modeling of EVs. Finally, we conclude and indicate directions for future work in section VII.

## II. Background

The impact of EV charging on the distribution system is an important and timely topic. Distribution grid operators will need to proactively prepare and dimension their grids based on realistic assumptions on the magnitude of the additional loading from EV charging.

Essential to quantifying the potential grid impacts is the coincidence factor (CF). According to the International Electrotechnical Commission (IEC), the CF is defined by "the ratio, expressed as a numerical value or as a percentage, of the simultaneous maximum demand of a group of electrical appliances or consumers within a specified period, to the sum of their individual maximum demands within the same period" [7]. Therefore the CF indicates the tendency of a set of loads to consume at the same time: for a lower CF, less grid capacity is required to serve the same set of loads. At the same time, an increase in CF may endanger grid security, and subsequently force grid reinforcement to happen early.

This story is further complicated by the muddling of the concept of CFs in distribution grid operation, where the CF in general use refers to the observed maximum load taken relative to the fuse size, instead of relative to the observed maximum power draw. In this way, CFs become a scaled proxy for total downstream load, rather than a strict measure of simultaneity.

When discussing CF, an important distinction should be made between small-scale, here meaning of order 50 units, and large-scale deployments. While the exact cut-off depends on the dynamics examined, due to reversion to the mean, the maximum observed load in large-scale deployments come primarily from coordinating factors such as the evening peak or price-following, while for small-scale deployments the maximum observed load is driven by stochastic uncertainty [8]. In deriving CFs, there is a fundamental difference in these two regimes, with the CFs for the small-scale regime primarily sensitive to the number of units considered and the probability of overlap of random fluctuations. This is particularly relevant for CFs arising from EVs, as the rollout of EVs on a feeder will be a gradual process, with long periods spent at low numbers of units and some feeders being small enough to never leave the small-scale regime.

Describing a realistic CF for EVs is complex as it depends on both technical and behavioral factors. Technical factors include the range of charging opportunities available to users, the size of the vehicle's battery and the charging power supported by charging equipment - all of which is subject to continuous development. Behavioral factors couple both to user psychology, where e.g. the impact of range anxiety may change as EVs become commonplace, and to market interactions, where several suggestions for so-called smart charging seek to distribute EV charging loads across the day through tariffs or incentives. We proceed to examine previous works in this area, to examine how CFs from EVs are represented in current literature.

### A. State of the art

As previously mentioned, behavioral factors are important to consider when investigating the CF of EV charging. In several studies, various behavioral factors are included when considering the user behavior for EV owners, however, the majority all have two factors in common: distance driven during a trip and the arrival time. Many of the studies including user behavior are primarily focused on investigating the grid impact of EVs. Such studies typically consider the distance driven and arrival time using a stochastic modeling approach [9–12]. In contrast, there are also studies focusing solely on the user behavior, and exploring other factors impacting the user behavior [13–19]. These studies explore factors such as different trip chains dependent on the EV owner's occupation [17, 18], social characteristics of EV owners [14], and plug-in probability curves [13, 19]. For the aforementioned studies, a mix of real-world or synthetic data is used to model user behavior. This paper uses the Danish National Travel Survey [20] to obtain a distribution for distance driven and arrival time at home. Further, plug-in probability curves based on real-world charging data are used [19].

A few studies are especially relevant for the present investigation as they include an explicit description of the CF for EVs.

In [15] Quirós-Tortós et al. utilize a dataset based on 221 residential EV users and more than 68,000 charging events. Probability density functions are generated for plug-in events

per day, start charging times and the SOC (beginning and end of charging session). Then a Monte Carlo approach is used to quantify a diversified peak demand for a different number of EVs. The CF is plotted for up to 200 EVs for both weekdays and weekend. The study finds that the CF will stabilize below 40% when exceeding 50 EVs and the paper quotes a CF of 33% for 1000 EVs. The calculation of the CF is based on the technical specifications of the Nissan Leaf with a rated charging power of 3.6 kW and 24 kWh batteries.

A study by Venegas et al. [21] uses a multi-agent EV model, a French survey and census data to analyze impacts of systematic and non-systematic charging in rural and urban distribution grids. Here systematic charging means that the EV is plugged in every night, regardless of SOC, while with non-systematic charging the EV is only plugged in when a low SOC necessitates a recharged. For systematic charging the paper finds a CF of 40% (which is quoted as a common recommendation for sizing in collective residential buildings in France) - but does not elaborate on the CF during non-systematic charging. The study concludes that non-systematic charging will generally reduce grid loading.

A study by Calearo et al. [22] proposed a method to generate individual charging patterns to quantify loading impacts on distribution grid feeders. The combined charging patterns are applied to a representative radially run, semi-urban low voltage grid. The study finds a CF of 45% for single-phase charging (3.7 kW), while this decreases to 25% for three-phase charging (11 kW). The decrease in CF means that even though charging power is tripled the combined peak only increases by 50%. The study concludes that for a 100% EV penetration scenario; single phase charging will cause undervoltages due to phase imbalance while three-phase charging may ultimately result in transformer/cable overloading.

The studies describing the CF of EVs have been found to include three types of inputs: number of EVs, battery size and charging power. Table I provides an overview of the inputs mentioned in a number of studies.

TABLE I: Studies of coincidence factors of EV charging.

| Study | | No. EVs | Battery Sizes [kWh] | Charging Powers [kW] |
|---|---|---|---|---|
| Calearo et al. | [22] | 20, 127 1000 | 40 | 3.7, 11 |
| Flammini et al. | [23] | | | 12 |
| Quirós-Tortós et al. | [15] | 1-1000 | 24 | 3.6 |
| Tong et al. | [24] | 20-10000 | | 2, 3, 6, 15 |
| Aunedi et al. | [25] | 1 - 54 | | 3.7, 14 |
| Thie et al. | [26] | 1-10 | | |
| Palomino et al. | [11] | 1-6 | | 6.6, 12.9, 19.2 |

### B. Research gaps

Table I illustrates that the number of EVs and charging power are commonly considered when defining the CF of EV charging. A few of the identified studies also describe the battery size of the EVs on which the CF is based. These inputs are shown to vary significantly between studies, which is also reflected in the obtained CFs. Several of the studies map the CF as a function of number of EVs. While this relationship typically follow the same trend, a rapidly decreasing CF as a function of an increasing number of EVs, the CF for a particular number of EVs is found to differ significantly between studies.

In other words, how many EVs will it take before the stochastic uncertainty of small-scale deployments is left behind.

As an example, a CF of 50% is found for 2-3 EVs in [11, 26], while the same CF is found for more than 10 EVs in [15, 25].

The inputs chosen are often informed by the particular trial from which the data is extracted (vehicle type, charging power, etc.) and the particular grid chosen as a case (number of vehicles on a feeder) - the CF's sensitivity to such inputs are typically not explored.

## III. Model inputs

### A. Model introduction

The approach to modelling the CF of EVs is illustrated in Fig. 1, which lists the relevant inputs and outputs of the model.

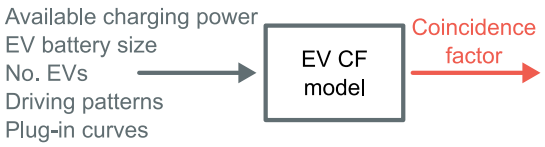


Fig. 1: Coincidence factor model overview.

We consider the following inputs, as they are expected to impact the CF for a given feeder:

- Available charging power.
- EV battery size.
- Number of EVs.

The specific values for battery sizes and charging power are based on expectations established together with the Danish EV industry [27], based on car models and charging equipment available presently and in the near future. The number of EVs is based on a danish low voltage distribution feeder, which generally has up to 100 customers connected. Therefore, the number of EVs considered ranges from 1 to 100.

The following factors must be handled by the modeling of each EV user's behavior:

- Driving patterns, i.e. time of arrival and daily energy use.
- Probability that the user plug-in upon arrival.
- Utilization of public charging infrastructure.

A major source of variation, which we do not examine in the present study is the composition of users on the feeder. That is, we do not explicitly address similarities in behavior shared by EV owners depending on their geographical location or other factors. However, except for these unaddressed dimensions the employed method allows robust calculation of CFs, which cover a wide range of possible combinations. In the course of the assays shown, we seek in particular to establish the sensitivity of the CF found on the model parameters listed above.

In order to combine these inputs to form CFs, we apply a Monte Carlo method, where a single CF is obtained for each set of inputs given. The procedure for obtaining a CF is as follows: First, many single-EV charging times series are generated, which are combined at random many times to cover a wide range of combinations. Then, from these many different combinations it is possible to obtain the CF. In the next section a single combination is referred to as a *run*, whereas a range of combinations are referred to as a *batch*. An example of such a single combination is shown in Fig. 2, which consists of 10 randomly selected single-EV charging time series. For each set of inputs a large pool of single-EV charging time series is generated, which ensures that a wide range of combinations can be achieved.

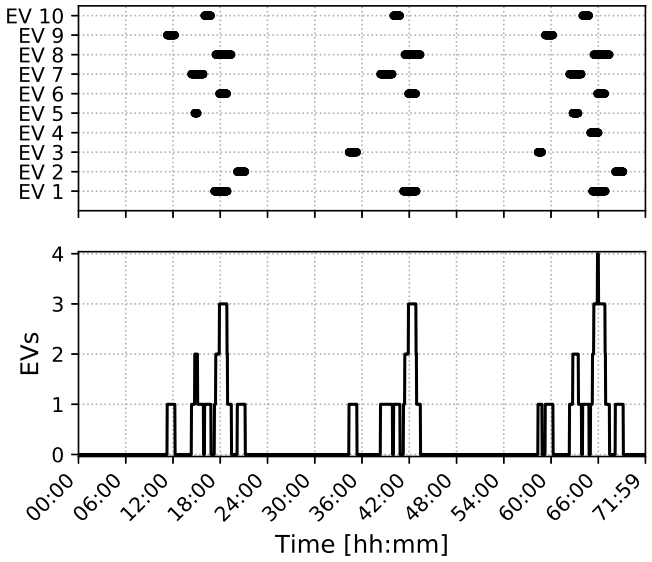


Fig. 2: Example of charging time series from the model with a length of 3 days and a specific set of inputs. (top) Single EV charging patterns with lines illustrating the charging duration of each EV; (bottom) Charging time series for a run of 10 EVs. Similar charging behavior is obtained if simulated for longer than 3 days.

This particular simulation lasts for 3 days, however, a similar charging behavior will be observed if simulated for longer than 3 days. Each EV charges at different times, and for different lengths of time, leading to the charging time series shown in the bottom plot of the figure. Since each CF is derived for their corresponding set of input parameters, then estimates for a particular feeder require the parameters of the model to be tuned in order to match the specific feeder's characteristic in terms of e.g. battery size and number of EVs on the feeder.

The following subsections provides an overview of the main inputs used for the modeling of CFs, while details on the generation of single-EV time series and the process of combining these time series is the topic of section IV.

### B. Inputs

*1) Driving behavior:* The driving behavior of this study is from a large interview-based travel survey - The Danish National Travel Survey (TU) [20]. This survey documents travel patterns of the Danish population and is maintained and developed by the Technical University of Denmark. Roughly 10,000 Danish citizens are interviewed each year, and this study has access to more than 160,000 of such interviews. Each interview contains a full account of the participant's travel activities for a single day, typically the one preceding the day of the interview.

Each journey of the day is described including departure time, arrival time, type of transportation, etc. Each interview is given a weight, which indicates to how many people this interview corresponds to in the entire population of Denmark. In this study only the interviews matching the following specifications have been selected:

- A passenger vehicle is the primary type of transportation during the journey.
- Only weekdays are considered - Mondays through Fridays.
- The journey starts and ends at the same location.

These specifications restrict interviews to those people who actively use their passenger cars during weekdays. The study focuses on weekdays, since this is where previous studies have found the largest CF to occur [25, 28]. From each interview satisfying the above specifications, the arrival time and distance driven in kilometers per day is used, which in this study is referred to as a driving behavior. The distribution for the arrival time and distance driven on weekdays is illustrated in Fig. 3.

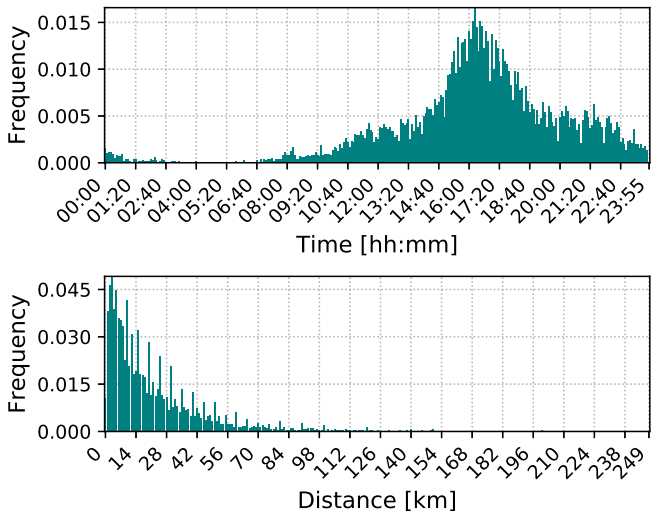


Fig. 3: Distribution of arrival time and distance driven on weekdays.

*2) Plug-in behavior:* The plug-in behavior is modeled by utilizing a plug-in probability curve based on a study carried out by Nissan – the study is based on the recorded behavior of more than 10,000 24 kWh Nissan Leafs, and express the probability that a plug-in will occur as a function of SOC

and daily driving distance [19]. There is a total of six plug-in curves used in this study where the main plug-in curve, referred to as P24 is based directly on the obtained results from the Nissan study as seen in Fig. 4. Whereas, P48L, P60L and P60R are extrapolations made by the authors based on P24 and described in Section III-B3. In addition, the two remaining plug-in curves, P24A and P60S, are based on always plugging in and keeping the plug-in curve for larger battery sizes identical with P24 based on the SOC, respectively.

P24 is illustrated in Fig. 4 with a different probability plug-in curve according to the average number of kilometers driven per day. An increase in kilometers driven increases the probability for the EV to plug-in upon arrival at home. The modelling of plug-in curves for increasing battery sizes and the implementation of the plug-in curve within the model is described in more detail in sections III-B3 and IV-B1, respectively.

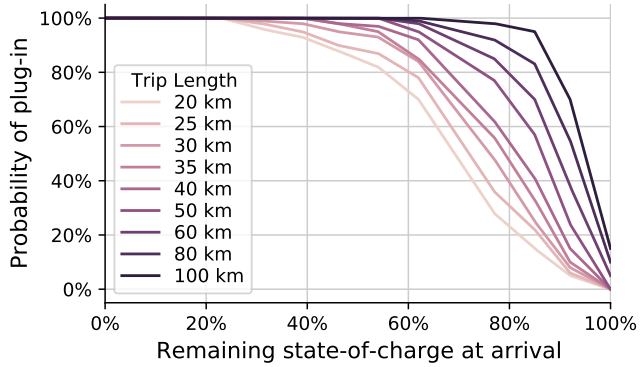


Fig. 4: Illustration of P24, which consists of a set of plug-in probability curves differing by the average kilometers driven [22, 29].

*3) Plug-in curves for larger battery sizes:* As part of the investigation, we wish to examine the impact on CF of cars with larger battery sizes, in particular 48 kWh and 60 kWh. However, the plug-in curves shown in Fig. 4 are derived for EVs with a battery size of 24 kWh. Thus, analogous curves are required for these larger battery sizes.

Fundamentally, extending the plug-in curve to higher battery sizes amounts to assuming how driver plug-in behavior changes in changing from a 24 kWh EV to a 60 kWh EV. Rather than proscribe a certain way to extend the plug-in curve, we proceed to examine the sensitivity of CFs to the choice of extension by examining scenarios corresponding to how driver plug-in behavior may change with higher battery sizes. In obtaining a larger capacity EV, the driver plug-in behavior may: (1) remain unchanged, (2) change toward a moderate increase in time between plug-in events, or (3) change to fully exploiting the increased battery capacity to minimize plug-in events. We model these changes by, respectively, *right shifting (R)* the plug-in curve, using the *same (S)* plug-in curve by SOC, or *left shifting (L)* the plug-in curve. As a final sensitivity factor, we include a plug-in curve where the driver *always (A)* plugs in.

The resulting plug-in curves are illustrated on Fig. 5, and listed in Table II.

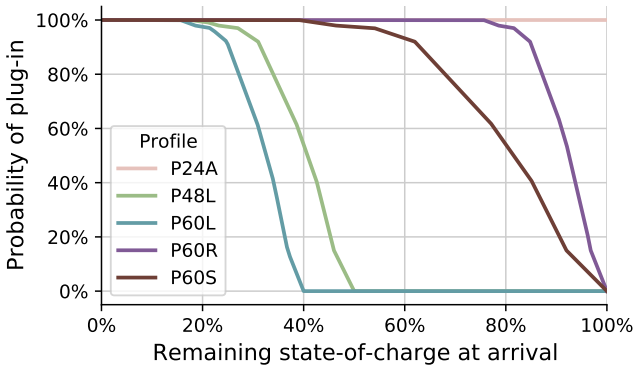


Fig. 5: Extrapolated plug-in curves for trips of 40 km at larger battery sizes. The curve for P24 overlaps the curve for P60S.

TABLE II: Plug-in curves extrapolated for larger battery sizes.

| Profile | Battery size | Curve based on |
|---|---|---|
| P24 | 24 kWh | Original data |
| P24A | 24 kWh | Always plug in |
| P48L | 48 kWh | Full use of extra range |
| P60L | 60 kWh | Full use of extra range |
| P60S | 60 kWh | Same as P24 by SOC |
| P60R | 60 kWh | No change in plug-in behavior |

While the true plug-in behavior for higher-capacity EVs may differ from those examined here, the chosen extensions cover most reasonable cases, and thus allow examining the sensitivity of our results to this choice.

### C. Definition of scenarios

We proceed to combine a plug-in curve, the rating of the EV charger, and the size of the EV battery to form the scenarios defined in Table III.

TABLE III: Selected simulation scenarios.

| Scenario | Profile | Charger Size [kW] | Battery Size [kWh] |
|---|---|---|---|
| S24O | P24 | 3.7 | 24 |
| S24B | P24 | 11 | 24 |
| S24D | P24 | 22 | 24 |
| S24A | P24A | 11 | 24 |
| S48L | P48L | 11 | 48 |
| S60L | P60L | 11 | 60 |
| S60S | P60S | 11 | 60 |
| S60R | P60R | 11 | 60 |

These scenarios are chosen to examine sensitivity to the various parameters as follows:

For the base scenario (S24B; ”base”), we take the case of a 24 kWh capacity EV connected to a 3-phase 16 A charger for a maximum charging power of 11 kW, and applying the P24 plug-in curve.

With respect to charging power, we choose to examine the cases of a 3.7 kW single-phase charger (S24O; ”one-phase”),

and the hypothetical case of using a three-phase 32 A charger, doubling the charging power of 22 kW total (S24D; "double") against the base scenario S24B.

By contrast, the choice of EV battery size cannot be cleanly separated from the choice of the plug-in curve, and we choose a three-tier strategy to handle this complication. First, the base scenario S24B is compared to a scenario where the EV always plugs in (S24A; "always"). Second, scenario S24B is compared to cases with $48\,\mathrm{kWh}$ and $60\,\mathrm{kWh}$ batteries, with the plug-in curve shifted to the left for each up-scaling (S48L, S60L; "left"). Finally, scenario S60L is compared to other scenarios with $60\,\mathrm{kWh}$ batteries, but where the plug-in curve is the same as P24 by SOC (S60S; "same") and shifted to the right (S60R; "right").

With the inputs and scenarios defined, we proceed to show the working of the simulation model.

## IV. Model Implementation

### A. Model overview

Our examination proceeds by generating synthetic time series of EV charging power for many synthetic feeders, and analyzing the statistics of the resulting charging time series to extract CFs for EV charging. Since the charging pattern of two different EVs on the same feeder are uncorrelated, i.e. any correspondence between departure time, trip length, arrival time and plug-in between neighbours is purely coincidental, we divide our model into two separate parts as illustrated in Fig. 6.

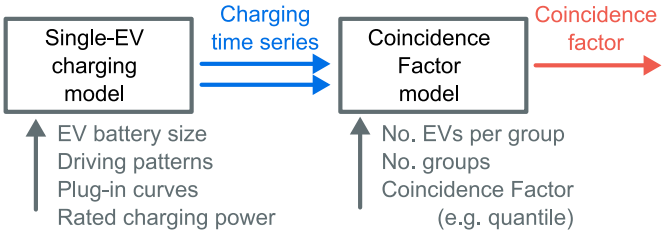


Fig. 6: Submodels for deriving coincidence factors.

First, charging time series for many individual EVs are generated. For each EV, this time series describes the power draw of the single charger mounted in the EV driver's residence. These single-EV charging time series form the charging pattern database. Examples of such single-EV charging time series are seen in Fig. 2 (top).

Second, a number of single-EV charging time series are randomly selected and combined to form the charging time series of the feeder defined as a *run r*. A batch containing a large number of independent runs is then analyzed to derive a CF. Fig. 2 (bottom) shows how the number of EVs charging simultaneously varies throughout a given run.

The generation of the charging pattern database is described in Subsection IV-B, while the method for deriving CFs is described in Subsection IV-C.

### B. Generation of single-EV charging time series

Each single-EV charging time series from the charging pattern database is generated based on the chosen EV battery capacity, charger power rating and a journey selected uniformly and randomly from the driving pattern database.

Depending on the EV's battery capacity and the chosen journey, a plug-in curve as illustrated in Fig. 4 and 5 is assigned. Each simulated EV is assigned a daily driving pattern, which is repeated every day in the simulated period. Given that the single-EV charging time series will be combined to form statistical aggregates, the re-use of journeys will be sufficiently mixed due to the large number of samples used to generate CFs.

The EV is initialized to have $SOC = 100\%$ at departure on day 1, and then follows the steps listed below for each day of the simulation:

- Reduce $SOC$ according to journey length (Subsection IV-B1)
- If $SOC$ is below a threshold, the EV partially charges using a public charger (Subsection IV-B2)
- The EV charges at home with a probability given by its $SOC$ according to the plug-in curve
- If the EV charges, $SOC = 100\%$ and the power signal is set equal the rated charging power for the duration of the charging (Subsection IV-B3)

The outcome is a charging time series of the power used by the charger at each time $t$, $P(t)$. Each charging time series is run for 60 days, of which the first 10 days are discarded before saving $P(t)$ in the charging pattern database. It was found that discarding 10 days is sufficient to achieve a stable distribution of SOCs across EVs, such that the initialization of all EVs at 100% SOC does not effect the results. The SOC of the individual EV is continuous over the simulation time, such that not charging on a given day increases the chance of charging on the following day.

*1) Daily energy use:* The energy usage during each journey $j$ is given by

$$\Delta SOC_j^{\mathrm{used}} = \frac{l_j}{\eta \cdot e_s}, \tag{1}$$

where $l_j$ is the journey's distance in km $e_s$ is the rated battery capacity of the EV in kWh during scenario $s$ and the performance $\eta$ of each EV is in this study defined as,

$$\eta = 5.7\ \frac{\mathrm{km}}{\mathrm{kWh}}. \tag{2}$$

The performance corresponds approximately to the battery-to-wheel efficiency of a Nissan Leaf, and is representative for mid-sized electric sedans available on the market today [30]. This study does not include charging efficiency. However, our choice of $\eta$ partially compensates for this; according to the database [30], wall-to-wheel performance at a $90\%$ wall-to-battery charging efficiency will result in a performance within the range, $4.7$ to $5.9\ \mathrm{km/kWh}$.

*2) Public charging:* If public charging is used, then upon arrival at home on day $d$, the SOC of the EV $v$ is given by

$$SOC_{v,d}^{\mathrm{arrival}} = SOC_{v,d}^{\mathrm{departure}} - \Delta SOC_j^{\mathrm{used}} + \Delta SOC_{v,d}^{\mathrm{offsite}}. \tag{3}$$

The amount recharged at the public charger is given by

$$\Delta SOC_{v,d}^{\text{offsite}} = E^{\text{offsite}} \cdot \left\lceil \frac{SOC^{\text{low}} - (SOC_{v,d}^{\text{departure}} - \Delta SOC_{j}^{\text{used}})}{E^{\text{offsite}}} \right\rceil, \quad (4)$$

where $\lceil x \rceil$ is the ceil operator.

*3) Plug-in rate and charging time:* At arrival on day $d$, a combination of $SOC_{v,d}^{\text{arrival}}$ and the plug-in curve for the EV gives the probability that the EV plugs in. The SOC at the beginning of the next day is then given as

$$SOC_{v,d+1}^{\text{departure}} = \begin{cases} SOC_{v,d}^{\text{arrival}} & \text{if EV does not charge} \\ 100\% & \text{otherwise} \end{cases}. \quad (5)$$

The time the EV $v$ spends charging is calculated as

$$\Delta t_{\text{charge}} = e_s \cdot \frac{1 - SOC_{v,d}^{\text{arrival}}}{r_s}, \quad (6)$$

where $r_s$ is the rated active power in kW of the charger and $e_s$ the rated battery capacity of the EV in kWh during scenario $s$.

Thus, for the given day $d$ where the EV $v$ is recharging, the charging power time series $P_v(t)$ is set equal to $e_s$ from $t = t_{\text{arrival}}$ to $t = (t_{\text{arrival}} + \Delta t_{\text{charge}})$.

### C. Calculation of the coincidence factor from charging time series

The charging time series contained in the charging pattern database are now combined to form a charging time series for the feeder. In a single run $r$, the total charging power time series of a feeder is defined as

$$P_r(t) = \sum_{v \in V_r} P_v(t), \quad (7)$$

where for each EV $v$ a charging pattern is sampled uniformly at random from the charging pattern database, until the required number of $M_b$ EVs on the feeder is reached. This process is repeated $N_{\text{runs}}$ times to form a *batch* $b$ consisting of $N_{\text{runs}}$ number of runs. The runs in each batch $b$ are subsequently analyzed to obtain CFs corresponding to the input parameters.

CFs are typically defined as the maximum observed total power consumption over the total of maximum power consumption [7]. However, due to the large amount of combinations examined, the model examined here can yield extremes which would be exponentially rare in the real world. Hence, the CFs derived would be overly conservative, and require excessive grid reinforcement when used to dimension real systems.

Instead of the maximum, we use high quantiles of the simulated charging power time series, which confers two major benefits: first, the quantiles correspond more closely to the typical high-load situations in the grid than the maxima, while their sensitivity to extreme events can be tuned through the quantile used. Second, a large part of sampling variance is eliminated, allowing for comparisons to use fewer batches as the statistics stabilize faster.

Here, we choose to cover 99.5% of the time $t \in T$ within each run and 99.5% of the runs $r \in R_b$ in a batch $b$. That is, for each batch $b$ we take the CF to be

$$cf_b = Q^{.995}\left(\left\{\frac{1}{M_b r_s} Q^{.995}\left(\{P_r(t) | \forall t \in T\}\right) | \forall r \in R_b\right\}\right), \quad (8)$$

where $Q^{.995}(\{\ldots\})$ denotes the .995 quantile over the given set, $r_s$ is the rated power of the charger and $M_b$ is the number of EVs in the batch. At the amount of runs and days per run considered here, the CFs found by (8) covers all but 1 hour of charging use over a 5-year period.

### D. Model fits

As a concise way of summarising the uncovered CFs, we report the parameters for a fit of the form

$$cf_s(M|k,\gamma,c) = k\frac{1}{M^{\gamma}} + c, \quad (9)$$

where $M$ is the number of EVs, $cf_s$ is the CF for scenario $s$, and $k$, $\gamma$ and $c$ are parameters to be fitted. Given a set of batches $b \in B_c$ of $M_b$ EVs each, we find parameters which minimize the sum of squared errors

$$SSE(k,\gamma,c) = \sum_{b \in B_c} \left(cf_s(M_b|k,\gamma,c) - cf_b\right)^2, \quad (10)$$

where $cf_b$ is the CF calculated from (8). The functional form of (9) is inspired by the scaling when $cf_b$ are sums of $N$ i.i.d. variables, for which one would find $cf(M) \propto M^{-\frac{1}{2}}$. In our fit, $c$ represents an additional saturation effect for high $M$. Other forms were tried, but (9) was found to give a good representation for the scenarios examined here.

## V. Results

### A. Determination of required number of runs per batch

The remaining undefined parameter is the number of runs, $N_{\text{runs}}$ in each batch. To determine this parameter, we generate batches with 100 EVs per feeder at increasingly larger number of runs until the inter-batch statistics stabilize. The $Q^{1.00}$ quantile across runs was considered to obtain stable statistics. Fig. 7 shows the statistics of the CF (8) for increasing $N_{\text{runs}}$, showing how the statistics stabilize after $N_{\text{runs}} = 1000$. Indeed, the results stabilize with a standard deviation of order $1\%$, corresponding to the inclusion or exclusion of a single EV at the time which sets the CF. We observed this stabilization also for lower numbers of EVs, and we keep $N_{\text{runs}} = 1000$ fixed for the remainder of the paper.

### B. Base scenario

Using this fixed number of runs, we proceed to run 5 batches at each of several number of EVs per batch, and fit the function (9) to these. The obtained CFs are illustrated in Fig. 8 along with the fit. For every scenario, there is a variation in the CFs found. This variation corresponds in each case to a difference

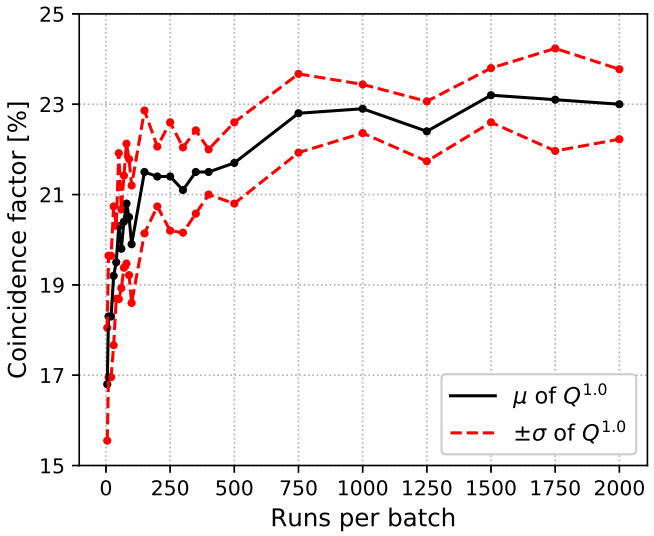


Fig. 7: Variation in coincidence factor across batches based on different number of runs. The mean and standard deviation of the maximum ($Q^{1.0}$) coincidence factor is shown for 10 batches of 100 EVs.

of an additional EV charging, when comparing the fit to the obtained CFs from the CF model as seen in Fig. 8. That is, CF fits for $M$ EVs have a sampling uncertainty of approximately $1/M$. For this and other scenarios, the fitted parameters for the CF as function of number of EVs is provided in Table IV.

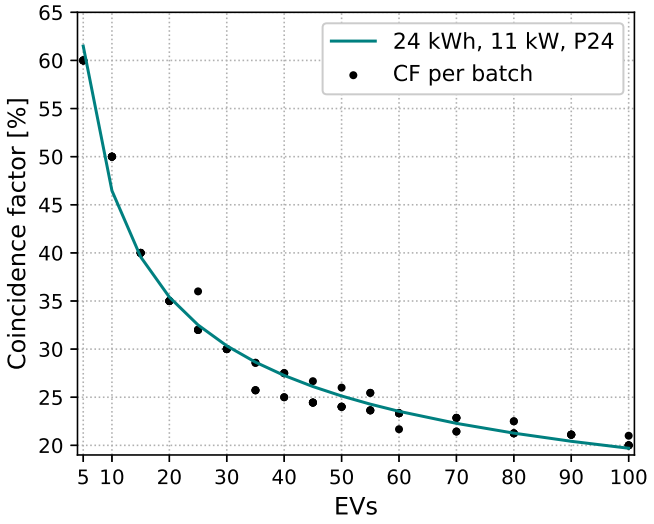


Fig. 8: Fitted model of coincidence factor for the base scenario, based on 5 batches per number of EVs.

### C. Sensitivity to charging power

The change in charging power has a significant effect on the CF, as seen in Fig. 9, which clearly indicates that EVs charging with a 11 kW charger, overlap less compared to EVs charging with a 3.7 kW. Especially at 100 EVs, there is close to a factor of 2 in difference between the two CFs for the two scenarios, or more precisely a difference of 16 percentage points. However, as seen the reduction in the CF is less when increasing the charging power from 11 to 22 kW. At 5 EVs the CF is fairly equal for both 11 and 22 kW, with a difference of around $1-2$ percentage points, however, for an increasing number of EVs the difference varies between $5-10$ percentage points. At 100 EVs there is a difference of 7 percentage points between 11 kW and 22 kW, which is close to a factor 2 in difference, similarly to the difference between 3.7 and 11 kW. However, the effect of increasing the charging power from 11 to 22 kW does not reduce the CF by a similar amount compared to the increase from 3.7 to 11 kW.

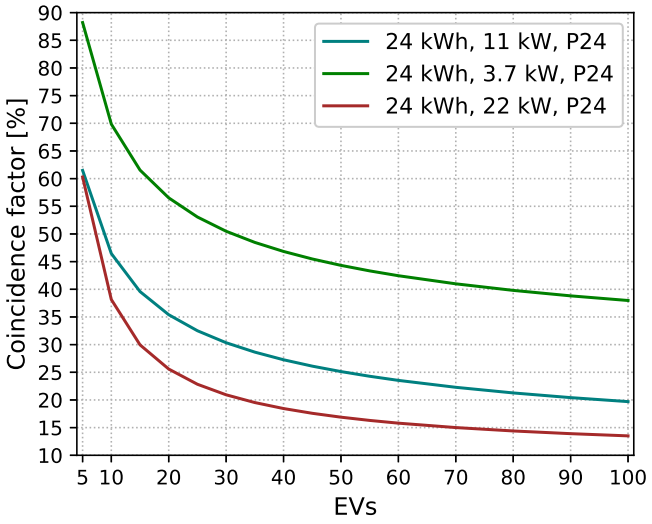


Fig. 9: The coincidence factor's sensitivity to a change in charging power.

### D. Sensitivity to battery size and plug-in curve

As seen in Fig. 10 the CF is less sensitive for a change in battery size, independent of the chosen plug-in curve. However, 60 kWh EVs still have the largest CF compared to the others, and from 24 kWh to 60 kWh at 100 EVs there is around 2 percentage points increase in the CF. Compared to the scenario using P24A, where the EVs plug-in every day upon arrival then the CF does not increase by much and still remains below P48L and P60L, and only 1 percentage point above P24 at 100 EVs. In addition, a plug-in curve, P24A, with a plug-in rate of 1, independent of the remaining SOC upon arrival at home has been included as a reference plug-in curve. P24A can be considered as an extreme plug-in curve, however, despite this it results in a similar CF as for the other plug-in curves. As seen in Fig. 10 the other plug-in curves vary with around $\pm 1$ percentage point around P24A at 100 EVs.

### E. Sensitivity to plug-in curve choice for higher kWh EVs

Finally, we examine the dependency on the choice of the plug-in curve. Fig. 11 shows the fits obtained by varying the plug-in curve for a 60 kWh capacity EV connected with an

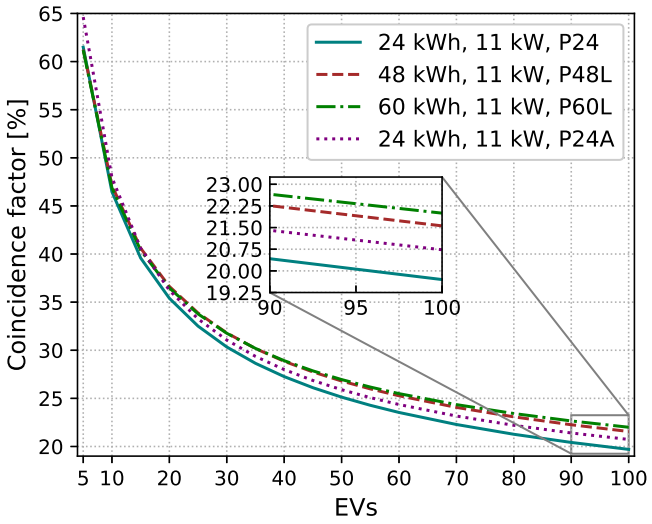


Fig. 10: Sensitivity to a change in battery size and plug-in curve.

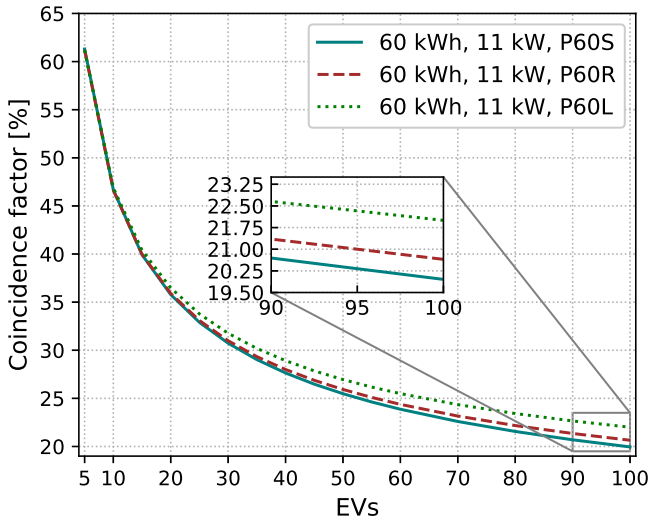


Fig. 11: Sensitivity to plug-in curves used for 60 kWh EVs.

TABLE IV: Fitted parameters for coincidence factor $cf$ as function of number of EVs according to (9).

| Profile | Battery size | Charger size | $\hat{\gamma}$ | $\hat{c}$ | $\hat{k}$ |
|---|---|---|---|---|---|
| P24 | 24 kWh | 3.7 kW | 0.460 | 21.11 | 140.90 |
| P24 | 24 kWh | 11 kW | 0.442 | 4.55 | 115.98 |
| P24 | 24 kWh | 22 kW | 0.816 | 9.07 | 190.57 |
| P24A | 24 kWh | 11 kW | 0.508 | 8.50 | 127.23 |
| P48L | 48 kWh | 11 kW | 0.430 | 6.47 | 109.51 |
| P60L | 60 kWh | 11 kW | 0.460 | 8.82 | 109.91 |
| P60R | 60 kWh | 11 kW | 0.441 | 5.89 | 112.53 |
| P60S | 60 kWh | 11 kW | 0.422 | 3.67 | 113.64 |

11 kW charger. A pairwise Student's T-test on the underlying batch results between S60R, S60S, and S60L reveal that for less than or approximately 50 EVs, these data can be taken as having a common mean. Above 50 EVs, the test indicates a significant ($p < 0.01$) difference in means between the scenarios. While this difference is statistically significant, our results indicate that the choice of extension for plug-in curves at larger battery sizes has an impact on CF of less than 2 percentage points.

### F. Peak active power demand

While the focus of this study is primarily on the CF, it would be useful to understand the peak power drawn by a feeder in a given scenario. This is a step towards operationalizing the CF for planning and designing the electrical grid. We present the peak active power draw from all $M$ chargers on the feeder, defined as

$$P_s^{\text{peak}}(M) = M \cdot cf_s(M) \cdot r_s, \tag{11}$$

where $r_s$ is the rated charging power in kW and $cf_s$ is the CF for $M$ chargers for scenario $s$.

The peak active power draw is shown in Fig. 12. While 3.7 kW chargers have high CFs relative to their capacity, their overall grid impact is a third less than that of 11 kW chargers. By contrast, doubling the charging power from S24B to S24D only results in at most a 20% increase in peak active power draw.

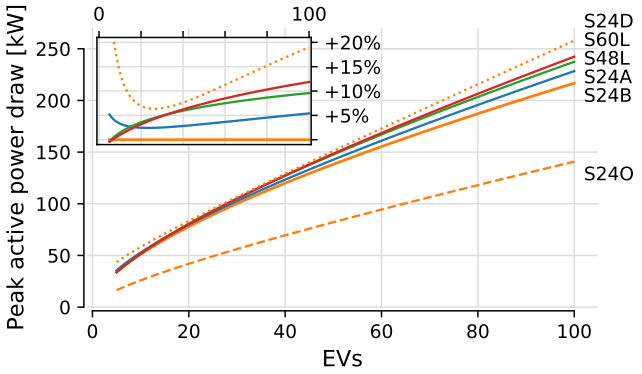


Fig. 12: Peak power draw from EV fleet by charger power. The inset shows peak charging power relative to S24B.

Further, the marginal increase in peak transformer power draw is greater with a small number of EVs, tailing off to a near-linear increase for more than approximately 35 EVs. Thus, a feeder will see a greater increase in peak power draw as the first few EVs are integrated, but the increase is lessened as additional EVs are added. This cautions against using linear models for predicting EV demand based on demand data when only a small number of EVs are present on the feeder, as peak charging power does not scale linearly below $\sim 50$ EVs.

### G. Scenario overview

Table V provides an overview of the key figures from the seven different scenarios. As seen between S24O, S24B and S24D as the CF decreases, then the peak power draw increases, hence illustrating the trade-off between reducing the CF by increasing the charging power. Additionally, the mean charging time for each EV reduces from around 3 hours

TABLE V: Scenario overview for 100 EVs.

| Scenario | S24O | S24B | S24D | S48L | S60L | S60S | S60R | S24A |
|---|---|---|---|---|---|---|---|---|
| Profile | P24 | P24 | P24 | P48L | P60L | P60S | P60R | P24A |
| Charger size [kW] | 3.7 | 11 | 22 | 11 | 11 | 11 | 11 | 11 |
| Battery Size [kWh] | 24 | 24 | 24 | 48 | 60 | 60 | 60 | 24 |
| Mean home charging events [events/(EV · 7 days)] | 4.30 | 4.30 | 4.30 | 1.66 | 1.21 | 3.21 | 4.31 | 7.0 |
| Mean public charging events [events/(EV · 7 days)] | 0.53 | 0.53 | 0.53 | 0.14 | 0.13 | 0.04 | 0.04 | 0.53 |
| Mean home charging time [min/(EV · day)] | 186.24 | 62.68 | 31.36 | 182.96 | 248.90 | 97.83 | 73.16 | 38.65 |
| Peak power draw [kW] | 133.2 | 220.0 | 286.0 | 242.1 | 253.0 | 220.0 | 231.1 | 231.0 |
| Coincidence factor [%] | 38.0 | 20.0 | 13.0 | 22.0 | 23.0 | 20.0 | 21.0 | 21.0 |

to 1 hour when increasing the charging power form 3.7 to 11 kW, and is further reduced to around 30 minutes when considering a 22 kW charger. In addition, as seen there is a clear difference in the mean home charging time and the plug-in frequency between the three plug-in curves, P60L, P60S and P60R, however, despite this difference they result in very similar CF.

### *H. Combinations of parameters*

The method as presented thus far has dealt with CFs defined from single parameter sets. Realistic scenarios will in general be based on different types of EVs, charger sizes and plug-in curves, all contributing to the overall CF. While a full treatment of such combinations is outside the scope of this paper, we note that our model may be extended to mixed models by altering how individual charging patterns are included in the CF calculation.

As an example of this alteration, we examine the effect of mixing 3.7 and 11 kW chargers in a certain proportion as seen in Fig. 13. Hence, this corresponds to a mix between scenario, S24O and S24B. The reason for using these two scenarios, is both because the majority of the studies presented in Table I primarily use chargers within this range, and the fact that there is the largest difference between these two scenarios' peak power draw and CF.

Fig. 13 shows that as the mix increasingly contain more 11 kW chargers, compared to 3.7 kW chargers, the CF decreases, and the peak power draw increases. As the percentage of 11 kW chargers in the mix increases, it approaches the known CF of 20% and the known power drawn of 220 kW. However, neither the CF or the peak power draw changes linearly, which is mostly dominant for the latter. This implies that a linear interpolation between the end points will not result in the correct peak power draw and CF for a given mix between the two scenarios, which is also seen from Fig 13, where the grey dashed line show the linear interpolation for the CF and peak power draw, respectively. Furthermore, as a result of this mixing, (11) is no longer valid, meaning the peak power draw must be obtained from the time series itself. Note that each data point in Fig. 13 is obtained from 5 batches, where each batch consists of 1000 runs and each run of 100 EVs.

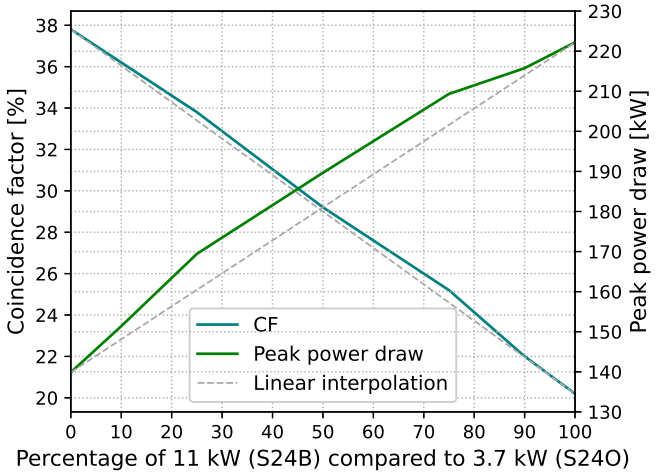


Fig. 13: Different combinations of scenario S24B and S24O with 100 EVs obtained from 5 batches. The x-axis indicates how many percent of the 100 EVs are based on S24B and the rest is based on S24O.

## VI. Discussion

For the scenarios where the charging power is kept constant, any change in the plug-in frequency is counteracted by a corresponding change in the charging duration, independently of the choice of the plug-in curve. This results in a CF with about 2 percentage points of variation across the different battery sizes, as seen in Table V.

By contrast, the CF is increased by about 16 and 23 percentage points if the charging power is reduced from 11 kW and 22 kW to 3.7 kW, respectively. However, when considering a 3.7 kW charger compared to a 11 kW and 22 kW charger the peak power demand is reduced by about 40% and 60%, respectively.

Further, we find that the aggregation effect at higher numbers of EVs is significant even for a relatively small number of EVs. At this point it is important to know if there are 20 or 25 EVs on a feeder, as it is to know the behaviors of their owners or the characteristics of the EV. The aggregation effect is primarily driven by different arrival times.

Increasing battery sizes reduce plug-in frequency from once every other day to once every fifth day, leading to reduced availability and thereby flexibility in the distribution network.

Therefore, if EVs should be a resource for grid flexibility, it may be necessary to incentivise users to plug-in their EVs regularly or otherwise alter their behavior. This has potential implications for future infrastructure upgrades in the distribution network.

It is currently unclear to which extent our sampling of journeys impacts our results. Since journeys from any part of the country are equally weighted, the set of journeys chosen for any given feeder may be more well-mixed than would be expected for any given area. There may be difference in driving patterns, e.g., between urban, sub-urban and rural grids, or in different regions, leading to greater homogeneity for journeys on any given feeder than found here. This would in turn entail a higher CF, as the aggregation effect due to variations in journeys would be less prominent.

## VII. Conclusion

By modeling driving behaviours of sets of EVs, we find that the coincidence factor is primarily influenced by the number of vehicles considered and, to a lesser degree, the supported charging power. A higher rated charging power will result in lower coincidence factors, but higher peak power draws. By contrast, including EV battery size and customer behavior are responsible for smaller corrections, of order $2\%$.

Coincidence factors are found to quickly decrease to below $30\%$ when considering a group of more than 30 vehicles, and less than $25\%$ when considering more than 50 vehicles for 11 kW charging. The uncovered coincidence factors are low compared to estimates in previous studies - especially considering that this represents near-worst-case scenarios based on a large number of combinations of behaviors.

For planning and design of the electrical grid when integrating electrical vehicles, it is important to have a proper understanding of the CF, in order to obtain the peak power drawn by the feeder. By using inputs valid for the given feeder, especially the number of customers connected and the charging power, it is possible to obtain a CF matching the particular feeder. Also, a trade-off between the cost of grid infrastructure and grid security can be made by adjusting the two quantiles. This paper decided to cover $99.5\%$ of the time in each run and $99.5\%$ of all the runs in the batch. However, depending on the requirement during planning it is possible to adjust these quantiles, and they can be adjusted independently of each other. Therefore, by lowering the quantiles a smaller CF can be obtained, which will imply a reduced infrastructure cost. As such, distribution system operators may use this study as part of their planning for integration of electric vehicles in the electrical grid. This is important as all European DSOs shall develop and publish biannual network development plans, which include requirements to the distribution system for connecting new loads including electric vehicles.

Future studies may focus on how controlled charging alters the coincidence factor, on the adverse effects that larger batteries may have on EV availability for grid services, i.e. fewer plugin events with a larger energy demand per event, or examine homogeneous compositions of EV owners which may increase the coincidence factor due to similarity in behavior. Furthermore, an extension of performing a sensitivity analysis on the wall-to-wheel efficiency and the inclusion of charging power curves.

## VIII. Acknowledgments

The authors would like to acknowledge the support of the EUDP funded projects ACES - Across Continent Electric Vehicle Services (grant EUDP17-I-12499, website: www.aces-bornholm.eu) and FUSE - Frederiksberg Urban Smart Electromobility (J.nr. 64020-1092, website: www.FUSE-project.dk). This study would not have been possible without data from The Danish National Travel Survey (tudata.dk), and we thank Hjalmar Christiansen from Center for Transport Analytics, DTU for support with extracting and understanding the data applied here.

## References

[1] Sandra Wappelhorst. The end of the road? an overview of combustion engine car phase-out announcements across europe. Technical report, 2020. https://theicct.org/sites/default/files/publications/Combustion-engine-phase-out-briefing-may11.2020.pdf.

[2] J. Coignard, P. MacDougall, F. Stadtmueller, and E. Vrettos. Will electric vehicles drive distribution grid upgrades?: The case of california. *IEEE Electrification Magazine*, 7(2):46–56, 2019. doi: 10.1109/MELE.2019.2908794.

[3] Simon Árpád Funke, Frances Sprei, Till Gnann, and Patrick Plötz. How much charging infrastructure do electric vehicles need? a review of the evidence and international comparison. *Transportation Research Part D: Transport and Environment*, 77:224–242, 2019. ISSN 1361-9209. doi: https://doi.org/10.1016/j.trd.2019.10.024. URL https://www.sciencedirect.com/science/article/pii/S136192091930896X.

[4] Katarina Knezovic. *Active integration of electric vehicles in the distribution network - theory, modelling and practice*. PhD thesis, 2017.

[5] Mattia Marinelli, Andreas Thingvad, and Lisa Calearo. *Across Continents Electric Vehicles Services Project: Final Report*. Technical University of Denmark, 2020.

[6] J. A. P. Lopes, F. J. Soares, and P. M. R. Almeida. Integration of electric vehicles in the electric power system. *Proceedings of the IEEE*, 99(1):168–183, 2011. doi: 10.1109/JPROC.2010.2066250.

[7] IEC. Coincidence factor definition. IEV ref: 691-10-03, 1973.

[8] M. Pertl, F. Carducci, M. Tabone, M. Marinelli, S. Kiliccote, and E. C. Kara. An equivalent time-variant storage model to harness ev flexibility: Forecast and aggregation. *IEEE Transactions on Industrial Informatics*, 15(4):1899–1910, 2019. doi: 10.1109/TII.2018.2865433.

[9] U. B. Irshad and S. Rafique. Stochastic modelling of electric vehicle's charging behaviour in parking lots. In *2020 IEEE Transportation Electrification Conference Expo (ITEC)*, pages 748–752, 2020. doi: 10.1109/ITEC48692.2020.9161566.

[10] A. B. Humayd and K. Bhattacharya. Design of optimal incentives for smart charging considering utility-customer interactions and distribution systems impact. In *2018 IEEE Power Energy Society General Meeting (PESGM)*, pages 1–1, 2018. doi: 10.1109/PESGM.2018.8585785.

[11] A. Palomino and M. Parvania. Probabilistic impact analysis of residential electric vehicle charging on distribution transformers. In *2018 North American Power Symposium (NAPS)*, pages 1–6, 2018. doi: 10.1109/NAPS.2018.8600630.

[12] Q. Dang. Electric vehicle (ev) charging management and relieve impacts in grids. In *2018 9th IEEE International Symposium on Power Electronics for Distributed Generation Systems (PEDG)*, pages 1–5, 2018. doi: 10.1109/PEDG.2018.8447802.

[13] Z. Fotouhi, M. R. Hashemi, H. Narimani, and I. S. Bayram. A general model for ev drivers' charging behavior. *IEEE Transactions on Vehicular Technology*, 68(8):7368–7382, 2019. doi: 10.1109/TVT.2019.2923260.

[14] K. Chaudhari, N. K. Kandasamy, A. Krishnan, A. Ukil, and H. B. Gooi. Agent-based aggregated behavior modeling for electric vehicle charging load. *IEEE Transactions on Industrial Informatics*, 15(2):856–868, 2019. doi: 10.1109/TII.2018.2823321.

[15] J. Quirós-Tortós, L. F. Ochoa, and B. Lees. A statistical analysis of ev charging behavior in the uk. In *2015 IEEE PES Innovative Smart Grid Technologies Latin America (ISGT LATAM)*, pages 445–449, 2015. doi: 10.1109/ISGT-LA.2015.7381196.

[16] L. Dong, C. Wang, M. Li, K. Sun, T. Chen, and Y. Sun. User decision-based analysis of urban electric vehicle loads. *CSEE Journal of Power and Energy Systems*, 7(1):190–200, 2021. doi: 10.17775/CSEEJPES.2020.00850.

[17] Azhar Ul-Haq, Carlo Cecati, and Ehab El-Saadany. Probabilistic modeling of electric vehicle charging pattern in a residential distribution network. *Electric Power Systems Research*, 157:126–133, 2018. ISSN 0378-7796. doi: https://doi.org/10.1016/j.epsr.2017.12.005. URL https://www.sciencedirect.com/science/article/pii/S0378779617304765.

[18] D. Tang and P. Wang. Probabilistic modeling of nodal charging demand based on spatial-temporal dynamics of moving electric vehicles. *IEEE Transactions on Smart Grid*, 7(2):627–636, 2016. doi: 10.1109/TSG.2015.2437415.

[19] Andreas Thingvad, Lisa Calearo, Peter Andersen, Mattia Marinelli, Myriam Neaimeh, Kenta Suzuki, and Kensuke Murai. Value of v2g frequency regulation in great britain considering real driving data. pages 1–5, 09 2019.

[20] The danish national travel survey, center for transport analytics - transport dtu, tudata.dk, 2019. Data version: TU0618v2, Data period: $\geq$ 2012, weighted data according to SessionWeight, '10-84 year olds'.

[21] Felipe Gonzalez Venegas, Marc Petit, and Yannick Perez. Impact of non-systematic electric vehicle charging behaviour on a distribution substation. 09 2019.

[22] Lisa Calearo, Andreas Thingvad, Kenta Suzuki, and Mattia Marinelli. Grid loading due to ev charging profiles based on pseudo-real driving pattern and user behaviour. *IEEE Trans. Transport. Electrific.*, 2019.

[23] Marco Giacomo Flammini, Giuseppe Prettico, Andreea Julea, Gianluca Fulli, Andrea Mazza, and Gianfranco Chicco. Statistical characterisation of the real transaction data gathered from electric vehicle charging stations. *Electric Power Systems Research*, 166:136 – 150, 2019. ISSN 0378-7796.

[24] Xin Tong, Chunlin Guo, Xiaoyan Yang, and Chenchen Chen. Research on characteristics of electric vehicle charging load and distribution network supportability. In *2016 IEEE PES Asia-Pacific Power and Energy Engineering Conference (APPEEC)*, pages 1539–1542, 2016.

[25] Marko Aunedi, Matthew Woolf, G. Strbac, Oloruntobi Babalola, and Michael Clark. Characteristic demand profiles of residential and commercial ev users and opportunities for smart charging. 06 2015.

[26] N. Thie, E. Junge, S. Hillenbrand, and M. Konermann. Evaluation of grid compatible load management concepts for e-mobility in distribution grids. In *2019 54th International Universities Power Engineering Conference (UPEC)*, pages 1–5, 2019.

[27] Søren Jakobsen, Lærke Flader, Peter Bach Andersen, Andreas Thingvad, and Jacob Bollerslev. Sådan skaber danmark grøn infrastruktur til én million elbiler, 2019.

[28] Jairo Quiros-Tortos, Luis(Nando Ochoa, and Becky Lees. A statistical analysis of ev charging behavior in the uk, 10 2015.

[29] Amaia González-Garrido, Andreas Thingvad, Haizea Gaztañaga, and Mattia Marinelli. Full-scale electric vehicles penetration in the danish island of bornholm – optimal scheduling and battery degradation under driving constraints. *Journal of Energy Storage*, 23:381–391, 2019. ISSN 2352-152X.

[30] EV Database. Electric vehicle database. https://ev-database.org, 2020.